SIMULATION OF THE MAGNET ERROR CORRECTION FOR THE SUPER TAU-CHARM FACILITY COLLIDER RINGS

J. Bao, P. Yang*, Y. Zou, L. Zhang, T. Liu, J. Tang
University of Science and Technology of China, Hefei, China

Abstract

Due to the complex optics and strong magnets of the Super Tau-Charm Facility (STCF) collider rings, the luminosity and beam dynamics are highly sensitive to magnetic field errors. Based on error sensitivity studies for the STCF and error tolerances adopted in other collider rings, a preliminary error budget has been established. This paper presents error correction results for STCF collider rings with center-of-mass energy of 2 GeV using a systematic correction chain, that includes first-turn trajectory correction, orbit correction via dispersion-free steering method, beta correction via LOCO method, and β_y^* correction with the k-modulation method. Simulation results show that after correction, the global closed orbit, β-beat, dispersion distortion, and coupling ratio are effectively reduced to acceptable levels. Consequently, the impact on nonlinear dynamics and luminosity is greatly suppressed.

INTRODUCTION

Aiming to investigate rich frontier physics in the tau-charm energy range and probe new physics beyond the standard model, the Super Tau-Charm Facility (STCF) [1, 2], proposed by the University of Science and Technology of China, is designed as a new-generation double-ring electron-positron collider. It covers a center-of-mass energy (CME) from 2 GeV to 7 GeV and reaches a high luminosity exceeding 1×10^{35} cm^{-2}s^{-1} at the optimal CME of 4 GeV. Table 1 summarizes the current main design parameters of the STCF collider rings with CME of 2 GeV. The previous magnet layout and linear optics performance of the collider rings (version 4) are presented in [1]. To reach such high luminosity, the collider adopts a large Piwinski angle and crab-waist collision scheme [3], similar to other e^+/e^- colliders including SuperKEKB [4], FCC-ee [5], CEPC [6] and BINP-SCTF [7].

Based on error sensitivity studies for STCF and the error tolerances adopted in other collider rings [8, 9], we have established a preliminary error budget, as summarized in Table 2. All errors are assumed to follow Gaussian distributions truncated at 2.5σ. The RMS horizontal and vertical misalignments of quadrupoles are generally 50 μm, with tighter tolerances of 30 μm applied to the quadrupoles in the final focus telescope section (Q_{FFT}) due to their higher sensitivity. Similarly, the RMS misalignments of sextupoles are 50 μm in the arc sections and 30 μm in the interaction region (IR). In this paper, we present the simulation of error correction for the STCF collider rings at a CME of 2 GeV, based on the version 5 lattice.

* penghui1@ustc.edu.cn

Table 1: Main Design Parameters of STCF Collider Rings at a CME of 2 GeV

Parameter	Value
Beam energy of single ring, E	1 GeV
Circumference, C	825.5 m
Natural emittance, ε_{nat}	3.25 nm
Coupling ratio, κ	1 %
Beta functions at IP, β_x^*/β_y^*	40 mm / 2 mm
Betatron tune, ν_x/ν_y	28.55 / 33.58
Beam current, I	0.8 A
Touschek lifetime τ	267 s
Luminosity, L	7.95×10^{33} cm^{-2}s^{-1}

Table 2: Magnet Error Budget of the STCF Collider Rings

Magnet	Misalignment			Rotation	Main field
	Δx (μm)	Δy (μm)	Δz (μm)	(mrad)	(%)
Dipole	100	100	100	0.1	0.02 %
Quadrupole	50	50	100	0.1	0.02 %
Q_{FFT}	30	30	100	0.1	0.02 %
Arc Sextupole	50	50	100	0.1	0.02 %
IR Sextupole	30	30	100	0.1	0.02 %

CORRECTION METHOD AND RESULTS

Correction System Layout and Correction Flow

Drawing on the experience gained from other collider rings, we outline the correction system layout as follows. Beam position monitors (BPMs) are placed in drifts adjacent to quadrupole magnets to allow beam-based alignment of their magnetic centres. Correctors are placed at locations with large beta functions: horizontally near focusing quadrupoles and vertically near defocusing quadrupoles. Sextupoles, which exhibit strong nonlinear magnetic fields, are equipped with both correctors and skew-quadrupole coils. To suppress the transverse coupling, additional dedicated skew quadrupoles are also installed in the long straight sections. Based on the error budget, 100 random error seeds are generated. To restore the orbits, linear optics, and other performance indicators, the following correction chain is performed for each seed: i) first turn trajectory correction; ii) closed orbit and dispersion correction; iii) linear optics and coupling correction; iv) β_y^* correction.

First-turn Trajectory Correction

The first-turn trajectory correction employs the trajectory response matrix and the singular value decomposition (SVD) method to steer the trajectory within the physical

aperture. Sextupoles and octupoles are switched off, and random errors are assigned to BPMs, including an offset error of 300 µm, a gain error of 5 %, a roll error of 0.1 mrad, and a noise error of 1 µm (all in RMS). About 25 % of the singular values are retained to avoid exceeding the corrector strength limits and to reduce the sensitivity to BPM errors. The simulation results show that after three to four correction iterations, the trajectories of all error seeds are generally reduced to below 5 mm, as shown in Fig. 1. The maximum corrector strength used in this step is approximately 0.3 mrad

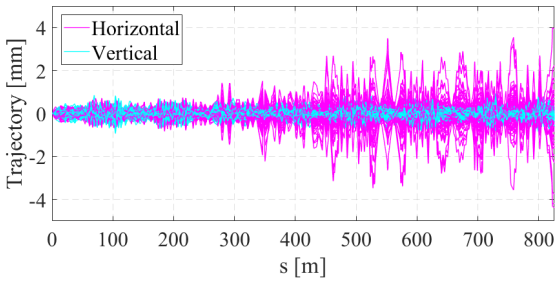

Figure 1: First turn trajectories after correction.

Closed Orbit and Dispersion Correction

The dispersion-free steering (DFS) method [10] effectively corrects the closed orbits and dispersions by solving

$$\mathbf{R}\vec{\theta} + \vec{d} = 0 \tag{1}$$

with

$$\mathbf{R} = \begin{pmatrix} (1-\alpha)\mathbf{A} \\ \alpha\mathbf{B} \end{pmatrix}, \quad \vec{d} = \begin{pmatrix} (1-\alpha)\vec{u} \\ \alpha\vec{D}_u \end{pmatrix} \tag{2}$$

where $\mathbf{A}$ and $\mathbf{B}$ are the response matrices of the orbit and dispersion with respect to the corrector kick, $\vec{u}$ the orbit vector, $\vec{D}_u$ the dispersion vector, and $\vec{\theta}$ the corrector strength. α is a weight factor; we found that $\alpha = 0.1$ provides a good balance between orbit and dispersion correction for STCF. In this correction step, the BPM offset error is reduced to 20 µm in RMS, assuming calibration has been performed. To further reduce the orbit at the IP, we assigned a larger weight to the BPMs near the IP. Figure 2 shows the orbit and dispersion distortions along the ring after correction. The maximum CODs are reduced from about 6 mm to below 600 µm, with RMS values of below 70 µm in both planes. The maximum dispersion distortion is about 5 mm, and the RMS distortion is below 0.7 mm in both planes. The maximum corrector strength used in this correction step is about 0.35 mrad, which remains feasible.

Linear Optics and Coupling Correction

The linear optics are corrected by tuning quadrupole strengths, and the transverse coupling is corrected using skew quadrupoles. To avoid the beta correction spoiling the results of the dispersion correction, the beta function and dispersion are corrected simultaneously. In this correction, the LOCO (Linear Optics from Closed Orbits) method [11]

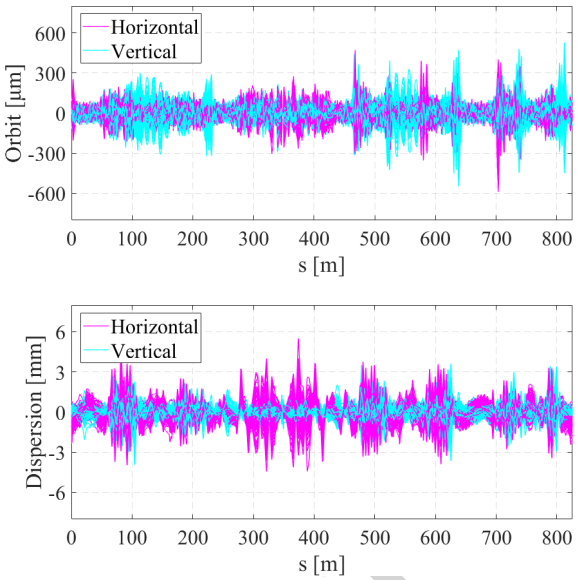

Figure 2: Closed orbits (up) and dispersion (down) distortions along the ring after correction.

is employed. The orbit response matrix (ORM) can be expressed as

$$\mathbf{M} = \begin{pmatrix} R_{xx} & R_{xy} \\ R_{yx} & R_{yy} \end{pmatrix}, \tag{3}$$

where R_{uv} represents the response of the orbit in the u-direction to a corrector kick in the v-direction. By fitting R_{xx} and R_{yy} of the error seeds to those of the ideal lattice, the β functions can be well recovered; by fitting R_{xy} and R_{yx} to zero, the transverse coupling is suppressed. In this fitting process, a least-squares method minimises the differences in matrix elements between each error seed and the ideal lattice. Figure 3 shows the β-beat along the ring after correction, excluding the β_y-beat at the IP. The global β-beat is reduced to less than 1 % RMS, while the β_y-beat at the IP remains large and requires additional correction. After correction, the natural emittance variation remains within 0.5 %, and the coupling ratio is reduced to below 0.1 %. The transverse tune shift is also well controlled, below 3×10^{-4}.

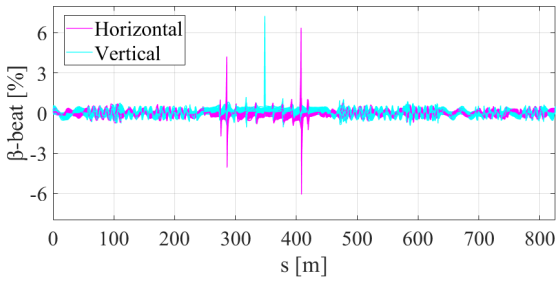

Figure 3: β-beat along the ring after correction, except the β_y-beat at IP.

β_y^* Correction

After LOCO correction, the β_y-beat at the IP cannot be reduced to an acceptable level. Therefore, we performed a dedicated correction for β_y at the IP by measuring β_y^* using

the k-modulation method [12]. By tuning the gradients of four or six quadrupoles near the IP to fit the β-beat of the error seed to that of the ideal lattice, the β-beat at the IP can be recovered to the ideal value. Taking one error seed as an example, Fig. 4 illustrates β_y near the IP before and after correction, demonstrating a good correction effect for β_y^*. After correction, the β_y-beat at the IP typically decreases to below 1 %, greatly reducing its impact on luminosity. Note that factors such as tune measurement accuracy and power supply jitter, which can affect the correction effectiveness, have not yet been taken into account in the current study.

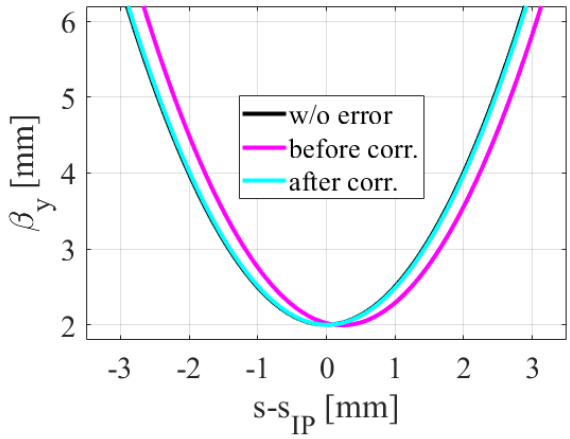

Figure 4: β_y near the IP before and after correction of one error seed.

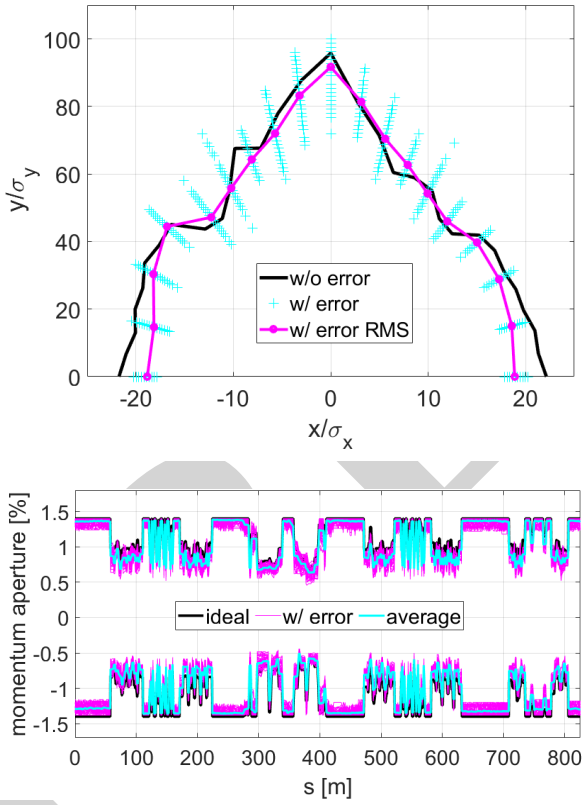

Figure 5: DAs (up) and MAs (down) of the ideal lattice and the error seeds after correction.

Figure 5 shows the dynamic apertures (DAs), normalized by the beam size, and the momentum apertures (MA) along the ring for the ideal lattice and the error seeds after correction. Simulation results show that the DAs are generally well recovered, reaching about $19\sigma_x$ and $92\sigma_y$ (RMS) in the horizontal and vertical planes, respectively. The MA exhibits a non-negligible decrease, which reduces the Touschek lifetime from 267 s for the ideal lattice to 191 s for the error seeds.

CONCLUSION

This paper presented simulations of error correction for the STCF collider rings at CME of 2 GeV. Systematic corrections greatly mitigate the impact of imperfections on luminosity and beam dynamics. After correction, the DA is well recovered, and the Touschek lifetime reaches about 72 % of the ideal value. In the next phase, the layout of BPMs and correction knobs will be refined through continuous iteration with lattice design and hardware. The error budget may be revised based on physical analysis and technical constraints, and disturbance factors such as measurement precision and power supply fluctuations will be taken into account for a more realistic assessment. These ongoing efforts are expected to further enhance the performance of the STCF collider rings under practical imperfections.

ACKNOWLEDGMENTS

This work was supported by the National Natural Science Foundation of China (No.12341501, No. 12405174). We also thank the Hefei Comprehensive National Science Center for the strong support on the STCF key technology research project.

REFERENCES

[1] X. Ai, L. An, S. An *et al.*, "Conceptual design report of the Super Tau-Charm Facility: the accelerator", *Nucl. Sci. Tech.*, vol. 36, p. 242, Dec. 2025. doi:10.1007/s41365-025-01833-x

[2] Y. Zou, L. Zhang *et al.*, "Optics design of the Super Tau-Charm Facility collider rings", *Nucl. Instrum. Methods Phys. Res. A*, vol. 1084, p. 171191, Apr. 2026. doi:10.1016/j.nima.2025.171191

[3] M. Zobov, D. Alesini, M. E. Biagini *et al.*, "Test of 'crab-waist' collisions at the DAΦNE Φ factory", *Phys. Rev. Lett.*, vol. 104, no. 17, p. 174801, 2010. doi:10.1103/PhysRevLett.104.174801

[4] Y. Ohnishi, T. Abe, K. Akai *et al.*, "SuperKEKB operation using crab waist collision scheme", *Eur. Phys. J. Plus*, vol. 136, no. 10, p. 1023, 2021. doi:10.1140/epjp/s13360-021-01979-8

[5] K. Oide, M. Aiba, S. Aumon *et al.*, "Design of beam optics for the Future Circular Collider e+e- collider rings", *Phys. Rev. Accel. Beams*, vol. 19, no. 11, p. 111005, 2016. doi:10.1103/PhysRevAccelBeams.19.111005

[6] J. Gao, *et al.*, "CEPC technical design report: Accelerator", *Radiat. Detect. Technol. Methods*, vol. 8, pp. 1-1105, 2024. doi:10.1007/s41605-024-00463-y

[7] A.Y. Barnyakov and Super Charm-Tau Factory collaboration, "The project of the Super Charm-Tau Factory in Novosibirsk", *J. Phys. Conf. Ser.*, vol. 1561, no. 1, p. 012004, 2020. doi:10.1088/1742-6596/1561/1/012004

[8] B. Wang, Y.Y. Wei, Y.W. Wang, C.H. Yu, Y. Zhang, "Imperfection and error correction for the CEPC CDR lattice", *Int. J. Mod. Phys. A*, vol. 37, no. 30, p. 2246005, 2022. doi:10.1142/S0217751X22460058

[9] S. S. Jagabathuni, F. Carlier, and S. Liuzzo, "FCC-ee optics tuning studies with pyAT and Xsuite", in *Proc. IPAC'25*, Taipei, Taiwan, Jun. 2025, pp. 394–397. doi:10.18429/JACoW-IPAC2025-MOPM037

[10] R. Assmann, P. Raimondi, G. Roy, J. Wenninger, "Emittance optimization with dispersion free steering at LEP", *Phys. Rev. ST Accel. Beams*, vol. 3, no. 12, p. 121001, 2000. doi:10.1103/PhysRevSTAB.3.121001

[11] J. Safranek, "Experimental determination of storage ring optics using orbit response measurements", *Nucl. Instrum. Methods Phys. Res. A*, vol. 388, no. 1, pp. 27-36, 1997. doi:10.1016/S0168-9002(97)00309-4

[12] F. Carlier, R. Tomás, "Accuracy and feasibility of the β^* measurement for LHC and High Luminosity LHC using k modulation", *Phys. Rev. Accel. Beams*, vol. 20, no. 1, p. 011005, 2017. doi:10.1103/PhysRevAccelBeams.20.011005